Earth and Planetary Science Letters 463 (2017) 127–135

Contents lists available at ScienceDirect

Earth and Planetary Science Letters

www.elsevier.com/locate/epsl

Magnesium isotopic variation of oceanic island basalts generated by partial melting and crustal recycling

Yuan Zhong [a], Li-Hui Chen [a,*], Xiao-Jun Wang [a], Guo-Liang Zhang [b,c], Lie-Wen Xie [d], Gang Zeng [a]

[a] State Key Laboratory for Mineral Deposits Research, School of Earth Sciences and Engineering, Nanjing University, Nanjing 210023, China
[b] Key Laboratory of Marine Geology and Environment, Institute of Oceanology, Chinese Academy of Sciences, Qingdao 266071, China
[c] Laboratory for Marine Geology, Qingdao National Laboratory for Marine Science and Technology, Qingdao 266000, China
[d] State Key Laboratory of Lithospheric Evolution, Institute of Geology and Geophysics, Chinese Academy of Sciences, Beijing 100029, China

ARTICLE INFO

Article history:
Received 30 November 2016
Received in revised form 25 January 2017
Accepted 29 January 2017
Available online xxxx
Editor: T.A. Mather

Keywords:
magnesium isotopes
oceanic basalt
partial melting
crustal recycling

ABSTRACT

Ocean island basalts (OIBs) are geochemically diverse in radiogenic isotopes, a feature that is commonly ascribed to record the chemical heterogeneity of their deep-mantle source, where significant compositional variation relates to variable amounts of ancient recycled crustal material. Although Mg is a major constituent of the mantle, it is still unclear whether Mg isotopes of OIBs predominantly correspond to deep-mantle source heterogeneity or processes such as partial melting. Here, we present Mg isotopic and trace-element compositional data for OIBs from the Hawaii islands, the Louisville seamounts, and for altered oceanic crust samples from the South Pacific. The δ^{26}Mg value range of these OIBs is -0.29 ± 0.07‰ (2SD, $n = 17$), which is a variation approximately twice as large as the known compositional variation of the peridotitic mantle (-0.23 ± 0.04‰, 2SD). Moreover, alkaline basalt (-0.31 ± 0.04‰, 2SD, $n = 12$) is relatively enriched in light Mg isotopes compared to tholeiitic basalt (-0.24 ± 0.02‰, 2SD, $n = 5$). In contrast, altered oceanic crust analyzed in this study has heavier Mg isotopic composition (-0.18 ± 0.08‰, 2SD, $n = 13$) relative to the basalts and to the peridotitic mantle. An evaluation of our and published data shows that the δ^{26}Mg values of most OIBs negatively correlate with melting-sensitive trace-element ratios, but that they are uncorrelated with source-sensitive elemental ratios. This implies that Mg isotopic variation in most OIBs is largely controlled by variable degrees of partial melting and not by source heterogeneity. Negative correlation between Nb/Zr (or La/Sm) versus δ^{26}Mg suggests that altered oceanic crust with heavier Mg isotopic composition is a more suitable source candidate for common OIBs. However, for a given melting degree, Louisville basalts have lower δ^{26}Mg values than other OIBs, suggesting a different source, e.g. a peridotitic mantle. Modeling calculations suggest that melting of both garnet pyroxenite (recycled altered oceanic crust) and garnet peridotite can generate melts with low-δ^{26}Mg signature for low-degree partial melting. Therefore, if the degree of partial melting can be independently constrained for the generation of parental OIB magma, the Mg isotopic compositions of their source can be estimated to investigate the chemical heterogeneity of the deep mantle.

1. Introduction

It is generally presumed that the highly variable radiogenic isotopic composition of ocean island basalt (OIB) is inherited from chemically heterogeneous deep mantle sources (Zindler and Hart, 1986; Hofmann, 1997; White, 2010, 2015). Trace-element ratios (e.g. Ce/Pb, Nb/U) and radiogenic isotopes (Sr, Nd, Pb and Hf) are commonly used to constrain the source heterogeneity of OIBs. However, whether magnesium isotopes (^{26}Mg, ^{25}Mg and ^{24}Mg) fingerprint such chemical heterogeneity in the deep mantle is still unclear, yet important to know, as magnesium is a major element in the mantle that provides an additional isotopic system for deciphering components and processes contributing to the diversity of OIBs.

To date, most studies have considered that mantle partial melting and basalt differentiation do not significantly fractionate Mg isotopes, given that stable isotope fractionation decreases as temperature increases (Urey, 1947). It is thus inferred that the Mg isotopic composition of mantle-derived rocks largely mirrors that

* Corresponding author.
E-mail address: chenlh@nju.edu.cn (L.-H. Chen).

http://dx.doi.org/10.1016/j.epsl.2017.01.040
0012-821X/

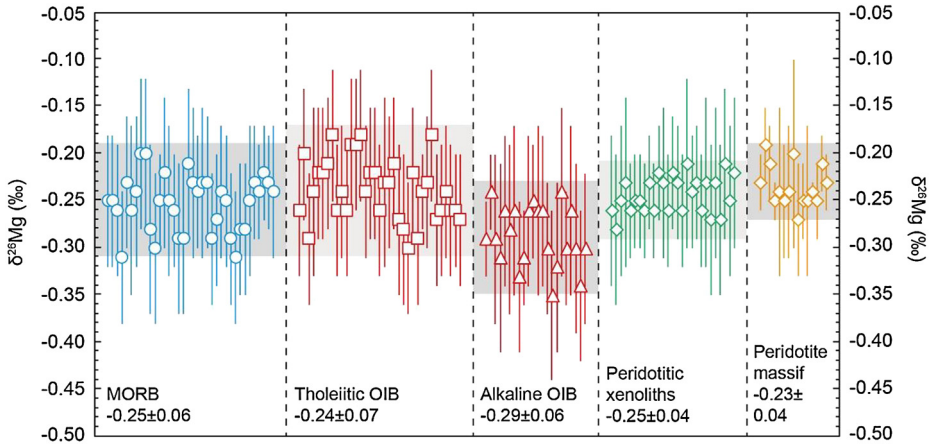

Fig. 1. Mg isotopic composition reported in the literature. The composition of oceanic basalt (MORB and OIB) and peridotite xenoliths were reported by Teng et al. (2010a). Based on these data, an average δ^{26}Mg value of -0.25 ± 0.07 (2SD) was proposed for the terrestrial mantle. It is notable that the peridotitic xenoliths investigated by most previous studies are from continental lithosphere, and they have experienced various degrees of metasomatism (also discussed in main text), therefore only the data from Teng et al. (2010a) were plotted. Lai et al. (2015) studied a suite of samples from the Horoman peridotite massif and suggested an average δ^{26}Mg value of -0.23 ± 0.04 (2SD) for pristine peridotitic mantle, which is more proper in comparison with the oceanic basalts. Gray fields are corresponding average values and 2SD uncertainties. Error bars represent 2SD uncertainties.

of their sources (Teng et al., 2007, 2010a). Using a set of global and geochemically diverse oceanic basalts and mantle peridotite xenoliths, Teng et al. (2010a) suggested that the Earth's mantle is homogeneous with an average δ^{26}Mg composition of -0.25 ± 0.07‰ (2SD), a chondritic value that is consistent with other published data (Handler et al., 2009; Yang et al., 2009; Young et al., 2009; Bourdon et al., 2010; Bizzarro et al., 2011; Huang et al., 2011; Pogge von Strandmann et al., 2011). However, the peridotitic xenoliths investigated by Teng et al. (2010a) are from continental lithosphere and have experienced various degrees of metasomatism, as well as in most other studies, e.g. Yang et al. (2009), Huang et al. (2011), Liu et al. (2011), Pogge von Strandmann et al. (2011) and Xiao et al. (2013). Therefore, the comparison between these xenoliths and OIB samples is not robust, as OIBs were generated in distinct oceanic settings. Recently, Lai et al. (2015) investigated the Mg isotopic composition of the Horoman Peridotite Massif, which is believed to be the remnants of pristine oceanic mantle. These samples are quite homogeneous in Mg isotopes with an average δ^{26}Mg composition of -0.23 ± 0.04‰ (2SD). While the known variation in δ^{26}Mg composition of OIBs and unmetasomatized peridotite is relatively small, all existing δ^{26}Mg data nevertheless show that OIBs are less homogeneous than the normal peridotitic mantle (Fig. 1). It is improbable that the discordance between the Mg isotopic composition of OIBs and peridotites results from analytical uncertainties, because students' *t*-tests show that there is no significant statistical difference between the mean δ^{26}Mg values of tholeiitic and peridotitic samples, but a significant and systematic difference (p-value $<<$ 0.01 at 95% confidence level) for tholeiitic and isotopically lighter alkaline OIBs. The objective of our study was to examine the origin of the δ^{26}Mg compositional variation between (1) OIBs and peridotite, as well as (2) alkaline and tholeiitic basalts. To achieve this objective, we have analyzed whole-rock Mg isotopic and trace-element composition of seventeen fresh OIB samples from the Hawaii islands and the Louisville Seamounts Chain, along with several altered oceanic crust samples from the Pacific.

2. Studied samples

The Hawaii and the Louisville Seamounts Chain are located in the northern and southern Pacific, respectively, and both are thought to have formed by deep-rooted mantle plumes (Courtillot et al., 2003) (Fig. S1). We have investigated ten samples from Hawaii and seven samples from the Louisville Seamounts Chain. The Hawaiian samples include tholeiitic shield-building lavas from Kilauea and Mauna Loa and alkaline basalts erupted from Hualālai Volcano. Our Louisville samples are all alkaline basalts, which were drilled at IODP sites U1372, U1373, and U1376 at the Canopus, Rigil, and Burton seamounts with average ages of 74.2 Ma, 69.5 Ma and 64.1 Ma, respectively (Koppers et al., 2012). In addition, altered ocean floor basalts were recovered at IODP sites U1365, U1367, and U1368 on the southern Pacific Plate (Fig. S1) (Zhang et al., 2012, 2013).

3. Experimental methods

3.1. Major- and trace-element analyses

Major-element composition of the OIB samples was determined on fused glass discs with a Thermo ARL 9900 X-ray fluorescence spectrometer (XRF) at the State Key Laboratory for Mineral Deposits Research, Nanjing University, China. Uncertainties were less than 2% for Si, Ti, Al, Fe, Mg and Ca, and less than 6% for Mn, K, Na and P as determined by comparison to the GSR3 rock standard. Trace-element composition of the Hawaiian samples was determined using an Agilent 7700x inductively coupled plasma mass spectrometer (ICP-MS) at Nanjing FocuMS Technology, China. The analyses of USGS rock reference materials (BHVO-2, BIR-1 and BCR-2) showed that analytical precision was better than 5% for Rb, Sr, Y, Zr, Hf, Nb, Ta, U, Th and the REEs, and 10% for Ba and Pb. Trace-element composition of the Louisville samples was determined using an ELAN 6100DRC ICP-MS at Northwest University, China. The analyses of USGS rock reference materials (BHVO-2, BCR-2 and AGV-2) equally yielded a precision better than 5% for Rb, Ba, Sr, Y, Zr, Hf, Nb, Ta, U, Th and the REEs, and 10% for Pb.

3.2. Mg purification and isotopic analysis

Mg isotopic analysis was performed at the Institute of Geology and Geophysics, Chinese Academy of Sciences, Beijing, following the procedures established and described in detail by An et al. (2014). All chemical preparation and analysis was carried out in an ultra-clean laboratory. Prior to column chemistry, approximately 20 mg of sample powders and 50 mg of USGS standard materials including BCR-2, BHVO-2, BIR-1 and GSP-2 were weighed in Savillex screw-top beakers and fully dissolved in a mixture of

Table 1
Measured magnesium isotopic composition of basalt samples.

	Sample name[a]	δ^{25}Mg[b]	2SD[c]	δ^{26}Mg	2SD	n[d]	Δ^{25}Mg′[e]
Altered oceanic crust	329-U1365E-2R-1-W 65/69	−0.086	0.026	−0.156	0.015	4	−0.004
	Replicate	−0.070	0.030	−0.149	0.024	4	+0.008
	329-U1365E-4R-2-W 88/92	−0.078	0.015	−0.149	0.025	4	+0.000
	329-U1365E-6R-2-W 99/103	−0.096	0.005	−0.189	0.042	4	+0.002
	329-U1365E-10R-1-W 46/50	−0.080	0.010	−0.169	0.020	4	+0.008
	329-U1365E-12R-1-W 19/23	−0.075	0.035	−0.154	0.021	4	+0.006
	329-U1367F-5R-1-W 36/39	−0.109	0.023	−0.207	0.024	6	−0.001
	329-U1367F-2R-3-W 43/47	−0.110	0.043	−0.198	0.027	4	−0.007
	Replicate	−0.099	0.020	−0.224	0.044	5	+0.018
	329-U1367F-6R-1-W 84/88	−0.101	0.012	−0.200	0.027	4	+0.004
	329-U1368F-4R-2-W 14/16	−0.110	0.051	−0.216	0.055	5	+0.003
	329-U1368F-5R-2-W 64/69	−0.034	0.035	−0.120	0.049	6	+0.028
	329-U1368F-7R-2-W 113/115	−0.122	0.045	−0.248	0.042	4	+0.007
	329-U1368F-11R-2-W 110/116	−0.072	0.033	−0.140	0.051	4	+0.001
	329-U1368F-14R-1-W 39/43	−0.070	0.025	−0.127	0.036	7	−0.004
	Average	−0.088	0.047	−0.175	0.076		
Hawaii tholeiitic	B-2	−0.103	0.023	−0.229	0.026	4	+0.016
	B-3	−0.118	0.036	−0.233	0.049	4	+0.004
	Replicate	−0.130	0.015	−0.255	0.039	4	+0.003
	H-4-1	−0.118	0.026	−0.243	0.047	4	+0.009
	H-9	−0.103	0.025	−0.246	0.045	4	+0.026
	N-1	−0.114	0.020	−0.234	0.025	4	+0.008
	Average	−0.111	0.015	−0.237	0.015		
Hawaii alkaline	K-1	−0.141	0.023	−0.296	0.040	4	+0.014
	K-2	−0.141	0.037	−0.295	0.033	5	+0.013
	K-3	−0.147	0.036	−0.288	0.033	5	+0.003
	K-4	−0.143	0.015	−0.289	0.015	4	+0.007
	K-5	−0.139	0.018	−0.294	0.015	4	+0.014
	Average	−0.142	0.006	−0.292	0.008		
Louisville alkaline	L02	−0.148	0.027	−0.311	0.045	6	+0.014
	L03	−0.163	0.014	−0.326	0.015	4	+0.007
	L06	−0.165	0.022	−0.315	0.033	4	−0.001
	L21	−0.172	0.020	−0.335	0.020	4	+0.003
	L22	−0.148	0.035	−0.315	0.027	4	+0.016
	Replicate	−0.157	0.042	−0.320	0.022	4	+0.009
	L23	−0.156	0.029	−0.329	0.042	4	+0.016
	L24	−0.147	0.047	−0.312	0.040	4	+0.015
	Average	−0.157	0.019	−0.320	0.019		

[a] Replicate represents the repeat of sample dissolution, column chemistry and instrumental analysis.
[b] Mg isotopic compositions are expressed in δ notation as per mil (‰) deviation from DSM-3 (Galy et al., 2003): $\delta^{X}Mg = [(^{X}Mg/^{24}Mg)_{sample}/(^{X}Mg/^{24}Mg)_{DSM\text{-}3} - 1] \times 1000$, where X equals 25 or 26.
[c] 2SD = 2 times the standard deviation of the population of n repeat measurements of a sample solution.
[d] Number of repeat measurements of each sample is denoted by "n".
[e] $\Delta^{25}Mg' = \delta^{25}Mg' - 0.521 \times \delta^{26}Mg'$, where $\delta^{X}Mg' = 1000 \times \ln[(\delta^{X}Mg + 1000)/1000]$ (Young and Galy, 2004).

concentrated HF–HNO_3 (~3:1, v/v). This initial digestion was evaporated to dryness and then treated with a mixture of concentrated HCl–HNO_3 and pure concentrated HNO_3, one or two times in sequence, to obtain completely clear solutions. The clear solutions, which contained about 20 μg Mg, were then dried and dissolved in 2N HNO_3 for column chemical analysis.

Mg purification was achieved by cation exchange chromatography in Savillex micro-columns loaded with 2 ml of Bio-Rad AG50W-X12 (200–400 mesh) pre-cleaned resin following established procedures (An et al., 2014). Prepared sample solutions were then loaded onto the resin twice with drying in between to obtain a pure Mg solution. The final reclaimed Mg solutions were dried and re-dissolved in 2% HNO_3, in preparation for mass spectrometry analysis. We also prepared a synthetic multi-element standard solution IGGMg1-A to examine the purification efficiency of the column. The Mg yields of all standards and unknown samples were ≥99.7% and the total procedural Mg blank during this study was less than 6 ng.

Mg isotopic composition was measured by the sample-standard bracketing method on a Thermo Neptune MC-ICP-MS in a medium-resolution mode. Sample and standard solutions were diluted to ~2 ppm Mg in the same batch of 2% HNO_3. The signal intensity for ^{24}Mg was generally about 4–5 V/ppm and the average blank contribution to this signal was less than 2 mV. To control analytical quality, each sample was measured at least 4 times and then averaged.

4. Results

The Mg isotopic composition of the measured samples is reported in Table 1, while data for the standard materials is presented in Table S1. The major- and trace-element composition of the samples is provided in Table S2. The 2SD long-term external precision was determined by repeated analyses of the international Mg standards (DSM-3 and Cambridge-1), in-house Mg standards (IGGMg1, IGGMg2 and SRM980), and various igneous rock standards (BCR-2, BHVO-2, BIR-1 and GSP-2). For δ^{26}Mg, the external precision is better than 0.06‰ (2SD). The internal precision on the measured ^{26}Mg/^{24}Mg composition based on ≥4 repeated analyses of the same solution during a single analytical session of this study is ≤0.05‰ (2SD). Repeated measurements of the Cambridge-1 and in-house Mg standard IGGMg1 at different dates yielded average δ^{26}Mg values of −2.60 ± 0.04‰ (2SD, n = 26) and −1.76 ± 0.04‰ (2SD, n = 70), respectively, which both agree with reported values (An and Huang, 2014; An et al., 2014). The results of multiple analyses of synthetic Mg

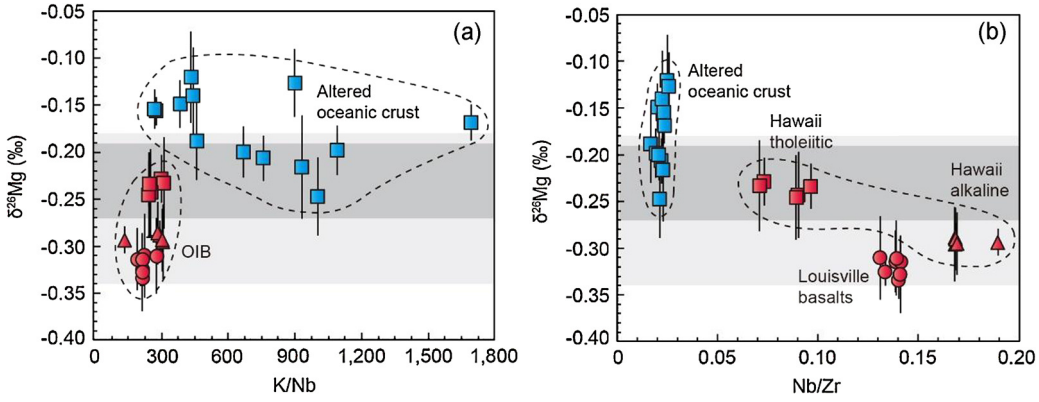

Fig. 2. Plots of δ^{26}Mg versus K/Nb and Nb/Zr. The dark gray field represents the range of peridotitic mantle composition suggested by Lai et al. (2015) with -0.23 ± 0.04‰ δ^{26}Mg (2SD). The light gray field represents the range of oceanic island basalt composition inferred by Teng et al. (2010a), which is -0.26 ± 0.08‰ δ^{26}Mg (2SD). Error bars represent 2SD uncertainties.

standard IGGMg1-A and USGS standard materials in this study are also in excellent agreement with those of An et al. (2014) and other previously published values within error.

All acquired Mg isotopic data fall along the mass-dependent fractionation line with a slope equal to 0.521 on the Mg three-isotope diagram (Fig. S2, for data see Table 1 and Table S1) (Young and Galy, 2004). Altered oceanic crust samples yield variable δ^{26}Mg values ranging from -0.25‰ to -0.12‰, and most are higher than those of reported peridotitic mantle compositions (Fig. 2). The composition of OIBs determined in our study have an average δ^{26}Mg value of -0.29 ± 0.07‰ (2SD, $n = 17$), which is identical to the average δ^{26}Mg value of OIBs (-0.26 ± 0.08‰, 2SD) reported by Teng et al. (2010a). These values overlap with but show a larger range than the δ^{26}Mg composition of the peridotitic mantle. Moreover, there are systematic and discernible differences between the Mg isotopic composition of tholeiitic and alkaline samples. The Hawaiian alkaline basalts have a lower average δ^{26}Mg value of -0.29 ± 0.01‰ (2SD, $n = 5$) than the Hawaiian tholeiitic lavas (-0.24 ± 0.02‰; 2SD, $n = 5$). The Louisville basalts have the lightest δ^{26}Mg values (average -0.32 ± 0.02‰; 2SD, $n = 7$). The tholeiitic δ^{26}Mg composition falls into the range of peridotitic mantle composition, while alkaline basalts are comparatively enriched in light Mg isotopes (Fig. 2).

5. Discussion

5.1. Mg isotopic composition of altered oceanic crust

The large range in K/Nb ratio (from 300 to around 1700) of our altered oceanic crust samples indicates affection of seawater alteration (Fig. 2). During alteration of basaltic glass to palagonite, a fraction of magnesium content is lost to the seawater, while the potassium content increases and Nb remains largely unmodified as a result of alteration (Staudigel and Hart, 1983). Heavy isotopes preferentially partition into weathered residues (e.g. the isotopic fractionation could up to 0.5‰ between primary rock and weathered residue) (Tipper et al., 2006; Pogge von Strandmann et al., 2008a, 2008b; Tipper et al., 2008; Teng et al., 2010b; Liu et al., 2014). We therefore link the high K/Na ratios and the heavy Mg isotopic signature to the presence of palagonite in the altered oceanic crust (AOC) samples. Secondary clay minerals are also usually K-rich and can take up isotopically heavy Mg (Huang et al., 2012). However, these clay minerals are much lower in MgO than basalt or palagonite. Considering an average δ^{26}Mg value of -0.83‰ for seawater (Ling et al., 2011), this then requires an isotopic fractionation much larger than 0.7‰ between clay minerals and seawater, which was not yet observed in nature. We therefore posit that the formation of palagonite dominantly accounts for the increase of both K/Nb ratios and δ^{26}Mg values in our AOC samples, and we further suggest that heavy Mg isotopic composition of AOC should be a common phenomenon. However, geochemical variation of oceanic crust induced by seawater alteration is complicated; consequently, we can hardly find a simple mixing trend between unaltered MORB and highly altered material.

5.2. Mg isotopic heterogeneity generated by partial melting

Previous interpretations have suggested that degree of partial melting and magma differentiation do not significantly fractionate Mg isotopes of basaltic melt (Teng et al., 2007, 2010a). Recycled AOC is, however, a common source component of OIBs. This conclusion was established on the ground of trace-element composition and Sr–Nd–Pb isotopic composition (Hofmann and White, 1982; Hofmann, 1997), and it may thus be suspected that OIBs have heavier Mg isotopic compositions than normal peridotitic mantle if recycled AOC carries its near-surface compositional signature into the mantle source. Intriguingly, this compositional signature has not been observed in our and other recent Mg isotope datasets (Fig. 1 and Fig. 2). On the contrary, alkaline OIBs have resolvably lighter Mg isotope composition than the peridotitic mantle. Light Mg isotopic composition of intraplate alkaline basalts has usually been attributed to recycled carbonate components in the mantle source (Yang et al., 2012; Wang et al., 2014), because carbonate has significantly lower δ^{26}Mg values (from -4.84‰ to -1.09‰) than other reservoirs (Galy et al., 2002; Young and Galy, 2004; Tipper et al., 2006; Geske et al., 2015). An additional or alternative, yet contested explanation is that variable degrees of mantle partial melting affect the Mg isotopic composition of their derived melts.

To evaluate if and to which degree partial melting and/or source-inherited composition account for the Mg isotopic heterogeneity in OIB samples, we now explore the possible links between a series of trace-element and δ^{26}Mg compositions. The considered trace-elemental ratios are either largely controlled by source composition or by the degree of partial melting. For elements with closely comparable compatibility, source composition largely controls their composition in the generated melt (e.g. Hf/Sm and Ba/Th). For elements with significantly different compatibility, variable degrees of partial melting will yield large variation in melt composition (e.g. Nb/Zr and La/Sm). Using this rationale, we have examined the potential correlations between δ^{26}Mg values and a series of trace-elemental ratios shown in Fig. 3 for our data and for oceanic basalt compositions reported by Teng et al. (2010a) (Table S3), which are Hawaiian tholeiitic basalts from the Koolau and Kilauea Iki lava lakes and alkaline basalts from Society Islands.

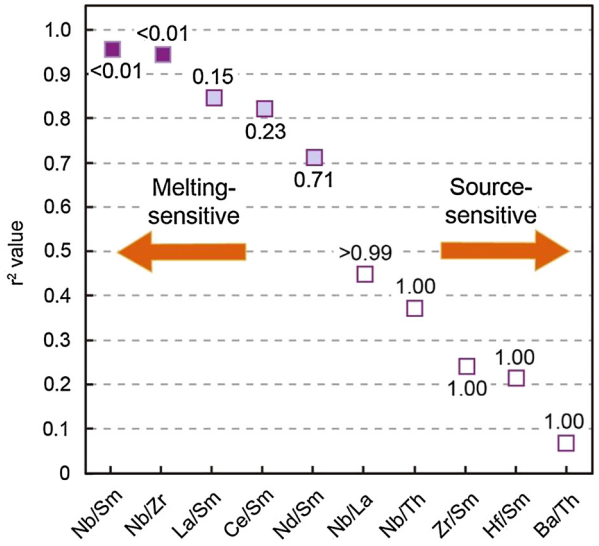

Fig. 3. Plot of correlation coefficients for δ^{26}Mg and characteristic elemental ratios. Figures inside the diagram are P values. The dark purple solid squares mark elemental ratios that show a significant variation with δ^{26}Mg at 95% confidence level ($P < 0.05$; further details can be found in Section 5.2 and Fig. S3). The white symbols mark elemental ratios that have P values close or equal to 1, thus lacking correlation with δ^{26}Mg. Light lilac squares have intermediate P values. Mg isotopic compositions are well correlated with trace-elemental ratios that are sensitive to partial melting (i.e. ratios on the left side of the figure). For δ^{26}Mg and trace-elemental ratios that are largely controlled by source composition, no significant correlation was found.

Because Teng et al. (2010a) have no matched trace-element composition in addition to their Mg isotopic data, we have selected and used trace-element data from the same locations and lithologies published by others. For each location, δ^{26}Mg values and trace-element ratios were averaged and corresponding 2SE were plotted.

The applied correlation analysis, i.e. a Monte Carlo analysis, is similar to the approach described by Li et al. (2016), which is able to account for and propagate uncertainties. In each simulation, a hypothetical dataset was generated by adding random normal distributed errors obtained from corresponding standard errors. The simulation was repeated 100,000 times, and regression coefficients including r^2 and p values were recorded for every run. The significance of the final regression results was judged by the fraction (P) of insignificant correlations ($p > 0.05$) among the 100,000 simulations. A P value <0.05 means that more than 95% of the simulated correlations were significant, i.e. the correlations between δ^{26}Mg and trace-elemental ratios are significant at 95% confidence level considering the uncertainty in the data.

Plots of average trace-element ratios versus δ^{26}Mg values for the OIBs are shown in Fig. S3 and their correlation coefficients are illustrated in Fig. 3. Excluding our Louisville samples, δ^{26}Mg values of OIBs are well correlated with their elemental ratios which are most sensitive to partial melting such as Nb/Zr and Nb/Sm ($r^2 > 0.90$ with $P < 0.01$). From the left side to right side of Fig. 3, decreasing r^2 and increasing P values indicate that correlations become insignificant. Meanwhile, there is no correlation between δ^{26}Mg values versus elemental ratios which are sensitive to source composition, e.g. Ba/Th, Zr/Sm and Hf/Sm. We therefore suggest that Mg isotopic heterogeneity and variation of most OIBs is linked to variable degrees of partial melting, rather than to source heterogeneity (e.g. variable contribution of recycled carbonate). Given that alkaline basalts are generally derived by lower degrees of source partial melting than tholeiitic basalts, we further propound that a higher degree of source partial melting leads to higher δ^{26}Mg values. Low-degree partial melting thus preferentially partitions light Mg isotopes into melts, while high-degree partial melting yields melt with Mg isotopic composition approaching the composition of protoliths.

5.3. Source influence on Mg isotopic heterogeneity

For a given La/Sm (or Nb/Zr) ratio, i.e. under similar melting degrees, the Louisville basalts always have a lighter Mg isotopic composition than other OIBs, suggesting that they have a unique source. Among all OIBs, the Louisville basalts are distinct with a homogeneous, FOZO-like Sr–Nd–Pb isotopic composition (Cheng et al., 1987; Beier et al., 2011; Vanderkluysen et al., 2014), while most other OIBs show a broad radiogenic Sr–Nd–Pb isotope range attributed to recycled oceanic crust and/or sediment in the source (Zindler and Hart, 1986; Weaver, 1991; Chauvel et al., 1992; Kogiso et al., 1997; Jackson et al., 2007). When oceanic crust is subducted into the mantle, it eventually transforms to garnet pyroxenite, which is the main source component for many typical OIBs, e.g. the shield-building basalts of Hawaii (Sobolev et al., 2005; Herzberg, 2006, 2011). Unlike these typical OIBs, the Louisville hotspot seems to tap a peridotitic source (Vanderkluysen et al., 2014), which may be in response to the thin lithosphere above the hotspot (Sobolev et al., 2007). Near the north end of the Louisville seamount chain a fossil spreading ridge, the Osbourn Trough, has been identified (Beier et al., 2011). The Louisville samples of this study were drilled at the northern end of this volcanic chain, representing the earliest magmatism (74.2 Ma–64.1 Ma) generated below a thinning lithosphere above the hotspot in the Mesozoic (Koppers et al., 2012). We therefore posit that a small or no contribution of pyroxenite-derived melt can explain the deviation of the Louisville basalts from other OIBs on the plots of δ^{26}Mg values versus melting-sensitive trace-element ratios.

5.4. Fractionation mechanisms during partial melting

Previous studies have established that variable degrees of partial melting or magmatic differentiation may fractionate stable metal isotopes, such as Fe, Zn and Ti (Williams and Bizimis, 2014; Doucet et al., 2016; Millet et al., 2016), depending on the residual and fractionating mineral assemblages. Recently, Schiller et al. (2017) found that the Mg isotopic composition of diogenite meteorites have heavier Mg isotope composition than eucrite meteorites, which can be attributed to extensive fractional crystallization of olivine and orthopyroxene. Since Mg in silicate melt appears to occur in five-fold coordination (Wilding et al., 2004; Henderson et al., 2006; Bajgain et al., 2015), while Mg in olivine and pyroxene occurs in six-fold coordination (Young et al., 2009; Schauble, 2011). The coordination difference leads to the enrichment of isotopically heavy Mg in residual melt, namely their diogenite samples.

The inference of Schiller et al. (2017) that high-degree fractionation leads to the enrichment of isotopically heavy Mg in the melt fraction is contrary to our interpretation that low-degree partial melting results in the formation of melt with a depletion in heavy Mg isotopes. A possible explanation for reconciling these apparently opposing interpretations is the distinct mineral assemblages with which the bulk melt being in equilibrium respectively. In the calculation of Schiller et al. (2017), only olivine and orthopyroxene were considered to crystallize. However, garnet is always an important phase in the source of OIBs regardless of whether the source is peridotitic or pyroxenitic. Since Mg is octahedrally coordinated in garnet, garnet is always enriched in light Mg isotopes compared to other coexisting silicate minerals (Huang et al., 2013). Melting experiments have found that garnet commences melting along with clinopyroxene at 3–4 GPa (Takahashi, 1986; Yasuda et al., 1994; Walter, 1998). Additionally, the melting reactions of MORB-like eclogite at 3 GPa reveal that the garnet

contribution diminishes significantly with increasing melt fraction (Pertermann and Hirschmann, 2003). Under such a circumstance, low-degree partial melts will inherit a stronger isotopic signature from garnet than high-degree partial melts, i.e. the light Mg isotopic composition of alkaline basalts could be reconciled with low-degree partial melting of a garnet-bearing source. Fractional crystallization and partial melting may thus form Mg isotopically light or heavy melt depending on the phase assemblage of the system. The effect is more significant for small-degree melting (large-degree crystallization) than large-degree melting (small-degree crystallization), which we further quantify below.

5.5. The effect of partial melting degree

Williams and Bizimis (2014) and Millet et al. (2016) have quantitatively evaluated the effect of variable degrees of partial melting on Fe and Zn isotopic fractionation, respectively. Here we follow the approach of Williams and Bizimis (2014), utilizing an incremental batch melting model for garnet pyroxenite and garnet peridotite, respectively, where the fractionation factors between melts and residue were recalculated at each step.

We have also followed Williams and Bizimis (2014) in their use of initial mineral modal abundance and melting mode for garnet pyroxenite. Initial mineral modal abundance and melting mode of garnet peridotite were taken from Davis et al. (2011) and Walter (1998), respectively. Clinopyroxene and garnet in peridotite were modeled to be exhausted around 30% degree of melting. Partition coefficients for garnet pyroxenite are from Pertermann et al. (2004), whereas those for garnet peridotite were calculated from Davis et al. (2011). The mass melted on each step was constantly set to 2% (F_0) of the bulk mass. Then the melting degree for the residue of each step n was calculated according to

$$f_n = \frac{F_0}{1-(n-1)F_0}$$

and the Mg abundance in the melt was modeled by using the equation of

$$c_n^{\text{melt}} = \frac{c_{n-1}^{\text{residue}}}{D_n + (1-P)f_n}$$

According to Williams and Bizimis (2014), the fractionation factor between the melt and the bulk residue can be obtained by

$$\alpha_{\text{melt-residue}} = \alpha_{\text{melt-cpx}} * \left(\sum_{i=1}^{n} [n_i \cdot \text{MgO}_{\text{mnr}}] / \sum_{i=1}^{n} [n_i \cdot \text{MgO}_{\text{mnr}} \cdot \alpha_{\text{mnr-cpx}}] \right)$$

where $\alpha_{\text{mnr-cpx}}$ is the fractionation factor between clinopyroxene and its co-existing mineral assemblage. For pyroxenite we directly estimated from published data of natural samples (Wang et al., 2012; Xiao et al., 2013) using

$$\delta_{\text{mineral}} - \delta_{\text{cpx}} = \Delta_{\text{mnr-cpx}} \approx 10^3 \ln \alpha_{\text{mnr-cpx}}$$

and for peridotite we use calculated theoretical values at 3 GPa and 1500 °C (Huang et al., 2013). $\alpha_{\text{melt-cpx}}$ is the fractionation factor between clinopyroxene and bulk melts. Contrary to the definitive $\alpha_{\text{mnr-cpx}}$, $\alpha_{\text{melt-cpx}}$ is a free variable due to the lack of experimental or theoretical constrains. Apparently, the value assigned to $\alpha_{\text{melt-cpx}}$ is crucial to the modeling result. Using the initial δ^{26}Mg value for clinopyroxene calculated by mass balance, we have then determined $\alpha_{\text{melt-cpx}}$ according to the difference between δ^{26}Mg values of clinopyroxene and our alkaline samples. This hypothetical $\alpha_{\text{melt-cpx}}$ is slightly lower than the calculated value, given that incipient melts should have lighter Mg isotopic composition than alkaline basalts. All fractionation factors are assumed to be constant during partial melting over the set intervals, following previous studies in this assumption. For garnet pyroxenite (recycled oceanic crust), we take the intersection point of δ^{26}Mg composition for AOC samples and typical OIBs in Fig. 2 as the initial Mg isotopic composition, namely −0.20‰. For garnet peridotite we use normal mantle value (−0.23%). Once the $\alpha_{\text{melt-residue}}$ was determined, δ_{melt} and δ_{residue} were calculated by mass balance. Details of the model parameters and calculation are presented in Table S4.

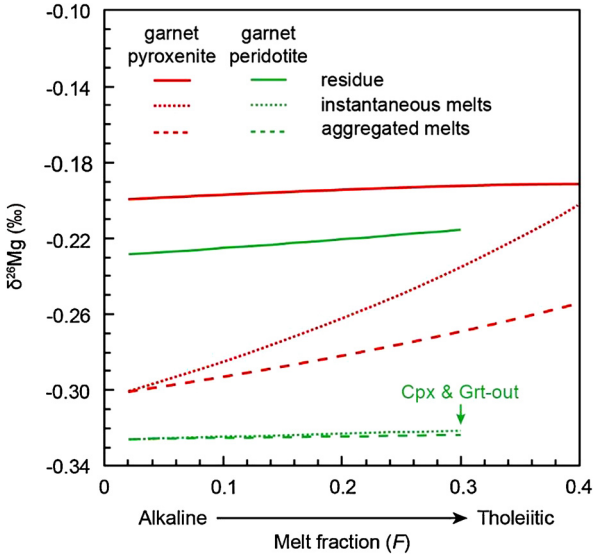

Fig. 4. Model δ^{26}Mg values calculated for melt and residue generated by fractional melting of garnet pyroxenite and garnet peridotite plotted against degree of partial melting. At low melt fractions, e.g. $F < 0.1$, melts are predicted to have significantly deviated composition, which is consistent with the observed offset between alkaline OIBs generated by low-degree partial melting and their mantle sources. It is notable that the Mg isotopic composition of the partial melting residue remains nearly constant with increasing degree of partial melting.

The model results are illustrated in Fig. 4. Partial melting of both mantle lithologies is modeled to result in significant δ^{26}Mg fractionation between residue and melt, reflecting the importance of high fractionation factor between garnet and coexisting silicate minerals (Huang et al., 2013), to which we refer as the "garnet effect". It is notable that peridotite-derived melts have light and constant Mg isotopic compositions, while the δ^{26}Mg values of pyroxenite-derived melts increase with their melting degrees. Such distinct fractionation behaviors are likely attributed to their different residual mineral assemblages in partial melting. In the melting reaction of peridotite, garnet and clinopyroxene will be consumed and orthopyroxene will be formed. The newly generated orthopyroxene is able to buffer relatively heavy Mg isotopes from melts, and consequently stabilize the relatively light Mg isotopic compositions of the latter. Nevertheless, for both lithologies, the difference between δ^{26}Mg values of melts and residue could reach an extreme value around 0.1‰, which is sufficient to account for the observed isotopic fractionation in OIB samples. We therefore conclude that variable degrees of partial melting of a garnet-bearing source (peridotitic or pyroxenitic) may explain the range of δ^{26}Mg values reported for OIBs. Moreover, given that most Mg stays in the source residue, the δ^{26}Mg value of the residue remains close to that of the primary source. This is consistent with the finding of previous studies that the differentiated upper mantle has a near-chondritic Mg isotopic composition (Handler et al., 2009).

5.6. Implications for the source heterogeneity of intraplate basalts

As discussed above, Hawaiian basalts have a typical pyroxenitic source whereas Louisville basalts have a unique peridotitic source.

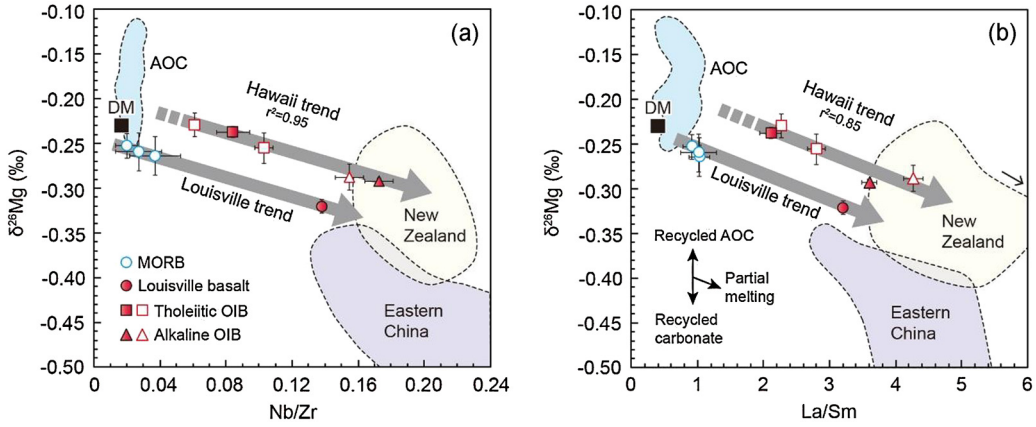

Fig. 5. Correlation of Nb/Zr and La/Sm vs. δ^{26}Mg values for intraplate basalts from various locations worldwide. White symbols represent samples from Teng et al. (2010a) (for details see Fig. S3 and Table S3). Data for eastern China basalts are from Yang et al. (2012) and Huang et al. (2015). Data for New Zealand basalts are from Wang et al. (2016), where we have only plotted the samples with an MgO higher than 5%. An average δ^{26}Mg value of −0.24‰ for depleted mantle (DM) was recalculated based on the Horoman peridotitic samples with Nb/Zr ratios lower than 0.04 (Takazawa et al., 2000; Lai et al., 2015). Fitting equations for Hawaii and Louisville trend are $y = -0.03x - 0.17$ and $y = -0.03x - 0.23$ in (a); and $y = -0.61x - 0.19$ and $y = -0.56x - 0.24$ in (b). Seawater alteration increases δ^{26}Mg values of oceanic crust samples. The Hawaii compositional trend reflects the presence of recycled oceanic crust in mantle source, representing "typical" OIB compositions. The Louisville basalt, as well as typical MORB, in contrast, are derived from low-δ^{26}Mg sources, yet may lie along a trend parallel to that of the Hawaiian samples. Error bars represent 2SE uncertainties.

Typical OIBs define a well-correlated trend for δ^{26}Mg and trace-element ratios (termed the "Hawaii trend") controlled by the degree of partial melting (Fig. 5). If we assume a parallel correlation trend (termed the "Louisville trend"), yet shifted to lower δ^{26}Mg, the composition of the Louisville basalt falls onto a trend with depleted mantle and MORBs, where MORBs and Louisville basalts represent products of high-degree and low-degree partial melting, respectively.

To further assess the effect of source compositional variation on Mg isotopic composition of intraplate basalts, we have also plotted data for intra-continental basalt from eastern China and New Zealand in Fig. 5. To minimize the effect of non-silicate mineral fractional crystallization on the composition of the New Zealand basalts, we have only used samples with MgO content higher than 5 wt%. The New Zealand basalts notably plot at the extensions of the Hawaiian fractionation trend, while the Eastern China basalts plot below the Louisville fractionation trends. However, basalts from both areas show a broad compositional range in δ^{26}Mg versus trace elements compared to the studied Hawaiian and Louisville basalts. The composition of the OIB-like basalts from Eastern China have been considered to reflect recycled carbonate in their source, given their distinct enrichment of highly incompatible elements and the depletion of Zr and Hf, together with their lower δ^{26}Mg and higher δ^{66}Zn values than peridotitic mantle (Zeng et al., 2010; Yang et al., 2012; Huang et al., 2015; Liu et al., 2016). For a given La/Sm or Nb/Zr ratio, for example, they have significantly lower δ^{26}Mg values than the Louisville basalts. Their source must therefore have a lighter Mg isotopic composition than the average peridotitic mantle. Previous studies have attributed this isotopically light Mg source to a stagnant slab in the mantle transition zone (Yang et al., 2012; Huang et al., 2015). The continental basalts from New Zealand are similar to basalts from eastern China in their La/Sm or Nb/Zr composition, whereas their δ^{26}Mg values are higher for a given trace element ratio. Wang et al. (2016) suggested a hybrid peridotitic and pyroxenitic source for the New Zealand alkaline basalts, where the end-member with low δ^{26}Mg composition was inferred to be recycled carbonate, which is also evident in the HIMU-like radiogenic isotopic affinities of these basalts (Hoernle et al., 2006; Timm et al., 2009, 2010). We therefore conclude that the difference in Mg isotopic compositions of continental basalts from eastern China and New Zealand, as well as those of the Hawaii and Louisville OIBs, is a response to the source heterogeneity *and* to variable degrees of partial melting of the common source types.

6. Summary and conclusions

The Mg isotopic composition of OIBs is variable. Mantle sources may differ in Mg isotopic composition, where variable amounts of recycled carbonate or altered oceanic crust yield sources with low or high δ^{26}Mg, respectively. Melts derived from variable sources inherit their Mg isotopic compositional variation, yet variable degrees of source partial melting also affect the Mg isotopic composition of the parental melts. In general, alkaline basalts derived by low-degree mantle melting have lower δ^{26}Mg values than tholeiitic basalts derived by high-degree mantle melting, and pyroxenite-derived basalts have higher δ^{26}Mg values than peridotite-derived basalts. In combination, Mg isotopic and trace-element composition can thus be used to identify deep mantle source heterogeneity (e.g. for the Hawaiian and Louisville OIBs) and variation in melting degree, e.g. through time, for common mantle sources tapped by common OIBs (e.g. for the Hawaii OIBs). To further exploit the information recorded by Mg isotopic composition of basaltic samples, future studies are needed that derive how Mg isotope partitioning between residue and melt at variable conditions of partial melting and for different phase assemblages.

Acknowledgements

Jin-Hui Yang and Yue-Heng Yang are acknowledged for their laboratory support. This work was supported by the National Natural Science Foundation of China (Grants 41372064 and 41376065). Wei-Qiang Li and Xiao-Ming Liu kindly provided constructive comments, and Gao-Jun Li offered generous help on statistical issues. Saskia Erdmann polished the manuscript. We appreciate constructive reviews from Dr. Philip Pogge von Strandmann and an anonymous reviewer, and the editorial work of Prof. Tamsin Mather.

Appendix A. Supplementary material

Supplementary material related to this article can be found online at http://dx.doi.org/10.1016/j.epsl.2017.01.040.

References

An, Y., Huang, F., 2014. A review of Mg isotope analytical methods by MC-ICP-MS. J. Earth Sci. 25, 822–840.

An, Y., Wu, F., Xiang, Y., Nan, X., Yu, X., Yang, J., Yu, H., Xie, L., Huang, F., 2014. High-precision Mg isotope analyses of low-Mg rocks by MC-ICP-MS. Chem. Geol. 390, 9–21.

Bajgain, S., Ghosh, D.B., Karki, B.B., 2015. Structure and density of basaltic melts at mantle conditions from first-principles simulations. Nat. Commun. 6, 8578.

Beier, C., Vanderkluysen, L., Regelous, M., Mahoney, J.J., Garbe-Schönberg, D., 2011. Lithospheric control on geochemical composition along the Louisville Seamount Chain. Geochem. Geophys. Geosyst. 12, Q0AM01. http://dx.doi.org/10.1029/2011GC003690.

Bizzarro, M., Paton, C., Larsen, K., Schiller, M., Trinquier, A., Ulfbeck, D., 2011. High-precision Mg-isotope measurements of terrestrial and extraterrestrial material by HR-MC-ICPMS—implications for the relative and absolute Mg-isotope composition of the bulk silicate Earth. J. Anal. At. Spectrom. 26, 565.

Bourdon, B., Tipper, E.T., Fitoussi, C., Stracke, A., 2010. Chondritic Mg isotope composition of the Earth. Geochim. Cosmochim. Acta 74, 5069–5083.

Chauvel, C., Hofmann, A.W., Vidal, P., 1992. HIMU-EM: the French Polynesian connection. Earth Planet. Sci. Lett. 110, 99–119.

Cheng, Q., Park, K.H., Macdougall, J., Zindler, A., Lugmair, G., Staudigel, H., Hawkins, J., Lonsdale, P., 1987. Isotopic evidence for a hotspot origin of the Louisville seamount chain. In: Seamounts, Islands, and Atolls, pp. 283–296.

Courtillot, V., Davaille, A., Besse, J., Stock, J., 2003. Three distinct types of hotspots in the Earth's mantle. Earth Planet. Sci. Lett. 205, 295–308.

Davis, F.A., Hirschmann, M.M., Humayun, M., 2011. The composition of the incipient partial melt of garnet peridotite at 3 GPa and the origin of OIB. Earth Planet. Sci. Lett. 308, 380–390.

Doucet, L.S., Mattielli, N., Ionov, D.A., Debouge, W., Golovin, A.V., 2016. Zn isotopic heterogeneity in the mantle: a melting control? Earth Planet. Sci. Lett. 451, 232–240.

Galy, A., Bar-Matthews, M., Halicz, L., O'Nions, R.K., 2002. Mg isotopic composition of carbonate: insight from speleothem formation. Earth Planet. Sci. Lett. 201, 105–115.

Galy, A., Yoffe, O., Janney, P.E., Williams, R.W., Cloquet, C., Alard, O., Halicz, L., Wadhwa, M., Hutcheon, I.D., Ramon, E., 2003. Magnesium isotope heterogeneity of the isotopic standard SRM980 and new reference materials for magnesium-isotope-ratio measurements. J. Anal. At. Spectrom. 18, 1352–1356.

Geske, A., Goldstein, R., Mavromatis, V., Richter, D., Buhl, D., Kluge, T., John, C., Immenhauser, A., 2015. The magnesium isotope (δ^{26}Mg) signature of dolomites. Geochim. Cosmochim. Acta 149, 131–151.

Handler, M.R., Baker, J.A., Schiller, M., Bennett, V.C., Yaxley, G.M., 2009. Magnesium stable isotope composition of Earth's upper mantle. Earth Planet. Sci. Lett. 282, 306–313.

Henderson, G.S., Calas, G., Stebbins, J.F., 2006. The structure of silicate glasses and melts. Elements 2, 269–273.

Herzberg, C., 2006. Petrology and thermal structure of the Hawaiian plume from Mauna Kea volcano. Nature 444, 605–609.

Herzberg, C., 2011. Identification of source lithology in the Hawaiian and Canary Islands: implications for origins. J. Petrol. 52, 113–146.

Hoernle, K., White, J.v., van den Bogaard, P., Hauff, F., Coombs, D., Werner, R., Timm, C., Garbe-Schönberg, D., Reay, A., Cooper, A., 2006. Cenozoic intraplate volcanism on New Zealand: upwelling induced by lithospheric removal. Earth Planet. Sci. Lett. 248, 350–367.

Hofmann, A., 1997. Mantle geochemistry: the message from oceanic volcanism. Nature 385, 219–229.

Hofmann, A.W., White, W.M., 1982. Mantle plumes from ancient oceanic crust. Earth Planet. Sci. Lett. 57, 421–436.

Huang, F., Chen, L., Wu, Z., Wang, W., 2013. First-principles calculations of equilibrium Mg isotope fractionations between garnet, clinopyroxene, orthopyroxene, and olivine: implications for Mg isotope thermometry. Earth Planet. Sci. Lett. 367, 61–70.

Huang, F., Zhang, Z., Lundstrom, C.C., Zhi, X., 2011. Iron and magnesium isotopic compositions of peridotite xenoliths from Eastern China. Geochim. Cosmochim. Acta 75, 3318–3334.

Huang, J., Li, S.-G., Xiao, Y., Ke, S., Li, W.-Y., Tian, Y., 2015. Origin of low δ^{26}Mg Cenozoic basalts from South China Block and their geodynamic implications. Geochim. Cosmochim. Acta 164, 298–317.

Huang, K.-J., Teng, F.-Z., Wei, G.-J., Ma, J.-L., Bao, Z.-Y., 2012. Adsorption- and desorption-controlled magnesium isotope fractionation during extreme weathering of basalt in Hainan Island, China. Earth. Planet. Sci. Lett. 359–360, 73–83.

Jackson, M.G., Hart, S.R., Koppers, A.A., Staudigel, H., Konter, J., Blusztajn, J., Kurz, M., Russell, J.A., 2007. The return of subducted continental crust in Samoan lavas. Nature 448, 684–687.

Kogiso, T., Tatsumi, Y., Shimoda, G., Barsczus, H.G., 1997. High μ (HIMU) ocean island basalts in southern Polynesia: new evidence for whole mantle scale recycling of subducted oceanic crust. J. Geophys. Res., Solid Earth 102, 8085–8103.

Koppers, A.A.P., Yamazaki, T., Geldmacher, J., Gee, J.S., Pressling, N., Koppers, A.A.P., Yamazaki, T., Geldmacher, J., Gee, J.S., Pressling, N., Hoshi, H., Anderson, L., Beier, C., Buchs, D.M., Chen, L.H., Cohen, B.E., Deschamps, F., Dorais, M.J., Ebuna, D., Ehmann, S., Fitton, J.G., Fulton, P.M., Ganbat, E., Hamelin, C., Hanyu, T., Kalnins, L., Kell, J., Machida, S., Mahoney, J.J., Moriya, K., Nichols, A.R.L., Rausch, S., Sano, S.I., Sylvan, J.B., Williams, R., 2012. Limited latitudinal mantle plume motion for the Louisville hotspot. Nat. Geosci. 5, 911–917.

Lai, Y.-J., Pogge von Strandmann, P.A.E., Dohmen, R., Takazawa, E., Elliott, T., 2015. The influence of melt infiltration on the Li and Mg isotopic composition of the Horoman Peridotite Massif. Geochim. Cosmochim. Acta 164, 318–332.

Li, G., Hartmann, J., Derry, L.A., West, A.J., You, C.-F., Long, X., Zhan, T., Li, L., Li, G., Qiu, W., 2016. Temperature dependence of basalt weathering. Earth Planet. Sci. Lett. 443, 59–69.

Ling, M.X., Sedaghatpour, F., Teng, F.Z., Hays, P.D., Strauss, J., Sun, W., 2011. Homogeneous magnesium isotopic composition of seawater: an excellent geostandard for Mg isotope analysis. Rapid Commun. Mass Spectrom. 25, 2828–2836.

Liu, S.-A., Teng, F.-Z., Yang, W., Wu, F.-Y., 2011. High-temperature inter-mineral magnesium isotope fractionation in mantle xenoliths from the North China craton. Earth Planet. Sci. Lett. 308, 131–140.

Liu, S.-A., Wang, Z.-Z., Li, S.-G., Huang, J., Yang, W., 2016. Zinc isotope evidence for a large-scale carbonated mantle beneath eastern China. Earth Planet. Sci. Lett. 444, 169–178.

Liu, X.-M., Teng, F.-Z., Rudnick, R.L., McDonough, W.F., Cummings, M.L., 2014. Massive magnesium depletion and isotope fractionation in weathered basalts. Geochim. Cosmochim. Acta 135, 336–349.

Millet, M.-A., Dauphas, N., Greber, N.D., Burton, K.W., Dale, C.W., Debret, B., Macpherson, C.G., Nowell, G.M., Williams, H.M., 2016. Titanium stable isotope investigation of magmatic processes on the Earth and Moon. Earth Planet. Sci. Lett. 449, 197–205.

Pertermann, M., Hirschmann, M.M., 2003. Anhydrous partial melting experiments on MORB-like eclogite: phase relations, phase compositions and mineral–melt partitioning of major elements at 2–3 GPa. J. Petrol. 44, 2173–2201.

Pertermann, M., Hirschmann, M.M., Hametner, K., Günther, D., Schmidt, M.W., 2004. Experimental determination of trace element partitioning between garnet and silica-rich liquid during anhydrous partial melting of MORB-like eclogite. Geochem. Geophys. Geosyst. 5, Q05A01. http://dx.doi.org/10.1029/2003GC000638.

Pogge von Strandmann, P.A.E., Burton, K.W., James, R.H., van Calsteren, P., Gislason, S.R., Sigfússon, B., 2008a. The influence of weathering processes on riverine magnesium isotopes in a basaltic terrain. Earth Planet. Sci. Lett. 276, 187–197.

Pogge von Strandmann, P.A.E., Elliott, T., Marschall, H.R., Coath, C., Lai, Y.-J., Jeffcoate, A.B., Ionov, D.A., 2011. Variations of Li and Mg isotope ratios in bulk chondrites and mantle xenoliths. Geochim. Cosmochim. Acta 75, 5247–5268.

Pogge von Strandmann, P.A.E., James, R.H., van Calsteren, P., Gíslason, S.R., Burton, K.W., 2008b. Lithium, magnesium and uranium isotope behaviour in the estuarine environment of basaltic islands. Earth Planet. Sci. Lett. 274, 462–471.

Schauble, E.A., 2011. First-principles estimates of equilibrium magnesium isotope fractionation in silicate, oxide, carbonate and hexaaquamagnesium (2+) crystals. Geochim. Cosmochim. Acta 75, 844–869.

Schiller, M., Dallas, J.A., Creech, J., Bizzarro, M., Baker, J.A., 2017. Tracking the formation of magma oceans in the Solar System using stable magnesium isotopes. Geochem. Perspect. Lett. 3, 22–31.

Sobolev, A.V., Hofmann, A.W., Kuzmin, D.V., Yaxley, G.M., Arndt, N.T., Chung, S.-L., Danyushevsky, L.V., Elliott, T., Frey, F.A., Garcia, M.O., 2007. The amount of recycled crust in sources of mantle-derived melts. Science 316, 412–417.

Sobolev, A.V., Hofmann, A.W., Sobolev, S.V., Nikogosian, I.K., 2005. An olivine-free mantle source of Hawaiian shield basalts. Nature 434, 590–597.

Staudigel, H., Hart, S.R., 1983. Alteration of basaltic glass: mechanisms and significance for the oceanic crust–seawater budget. Geochim. Cosmochim. Acta 47, 337–350.

Takahashi, E., 1986. Melting of a dry peridotite KLB-1 up to 14 GPa: implications on the origin of peridotitic upper mantle. J. Geophys. Res., Solid Earth 91, 9367–9382.

Takazawa, E., Frey, F.A., Shimizu, N., Obata, M., 2000. Whole rock compositional variations in an upper mantle peridotite (Horoman, Hokkaido, Japan): are they consistent with a partial melting process? Geochim. Cosmochim. Acta 64, 695–716.

Teng, F.-Z., Li, W.-Y., Ke, S., Marty, B., Dauphas, N., Huang, S., Wu, F.-Y., Pourmand, A., 2010a. Magnesium isotopic composition of the Earth and chondrites. Geochim. Cosmochim. Acta 74, 4150–4166.

Teng, F.-Z., Li, W.-Y., Rudnick, R.L., Gardner, L.R., 2010b. Contrasting lithium and magnesium isotope fractionation during continental weathering. Earth Planet. Sci. Lett. 300, 63–71.

Teng, F.-Z., Wadhwa, M., Helz, R.T., 2007. Investigation of magnesium isotope fractionation during basalt differentiation: implications for a chondritic composition of the terrestrial mantle. Earth Planet. Sci. Lett. 261, 84–92.

Timm, C., Hoernle, K., Van Den Bogaard, P., Bindeman, I., Weaver, S., 2009. Geochemical evolution of intraplate volcanism at Banks Peninsula, New Zealand: interaction between asthenospheric and lithospheric melts. J. Petrol. 50, 989–1023.

Timm, C., Hoernle, K., Werner, R., Hauff, F., van den Bogaard, P., White, J., Mortimer, N., Garbe-Schönberg, D., 2010. Temporal and geochemical evolution of the Cenozoic intraplate volcanism of Zealandia. Earth-Sci. Rev. 98, 38–64.

Tipper, E.T., Galy, A., Bickle, M.J., 2006. Riverine evidence for a fractionated reservoir of Ca and Mg on the continents: implications for the oceanic Ca cycle. Earth Planet. Sci. Lett. 247, 267–279.
Tipper, E.T., Galy, A., Bickle, M.J., 2008. Calcium and magnesium isotope systematics in rivers draining the Himalaya-Tibetan-Plateau region: lithological or fractionation control? Geochim. Cosmochim. Acta 72, 1057–1075.
Urey, H.C., 1947. The thermodynamic properties of isotopic substances. J. Chem. Soc. (Lond.), 562–581.
Vanderkluysen, L., Mahoney, J.J., Koppers, A.A., Beier, C., Regelous, M., Gee, J.S., Lonsdale, P.F., 2014. Louisville Seamount Chain: petrogenetic processes and geochemical evolution of the mantle source. Geochem. Geophys. Geosyst. 15, 2380–2400.
Walter, M.J., 1998. Melting of garnet peridotite and the origin of komatiite and depleted lithosphere. J. Petrol. 39, 29–60.
Wang, S.J., Teng, F.Z., Li, S.G., 2014. Tracing carbonate–silicate interaction during subduction using magnesium and oxygen isotopes. Nat. Commun. 5, 5328.
Wang, S.-J., Teng, F.-Z., Scott, J.M., 2016. Tracing the origin of continental HIMU-like intraplate volcanism using magnesium isotope systematics. Geochim. Cosmochim. Acta 185, 78–87.
Wang, S.-J., Teng, F.-Z., Williams, H.M., Li, S.-G., 2012. Magnesium isotopic variations in cratonic eclogites: origins and implications. Earth Planet. Sci. Lett. 359–360, 219–226.
Weaver, B.L., 1991. The origin of ocean island basalt end-member compositions: trace element and isotopic constraints. Earth Planet. Sci. Lett. 104, 381–397.
White, W.M., 2010. Oceanic island basalts and mantle plumes: the geochemical perspective. Annu. Rev. Earth Planet. Sci. 38, 133–160.
White, W.M., 2015. Probing the Earth's deep interior through geochemistry. Geochem. Perspect. 4.
Wilding, M.C., Benmore, C.J., Tangeman, J.A., Sampath, S., 2004. Evidence of different structures in magnesium silicate liquids: coordination changes in forsterite-to enstatite-composition glasses. Chem. Geol. 213, 281–291.
Williams, H.M., Bizimis, M., 2014. Iron isotope tracing of mantle heterogeneity within the source regions of oceanic basalts. Earth Planet. Sci. Lett. 404, 396–407.
Xiao, Y., Teng, F.-Z., Zhang, H.-F., Yang, W., 2013. Large magnesium isotope fractionation in peridotite xenoliths from eastern North China craton: product of melt–rock interaction. Geochim. Cosmochim. Acta 115, 241–261.
Yang, W., Teng, F.-Z., Zhang, H.-F., 2009. Chondritic magnesium isotopic composition of the terrestrial mantle: a case study of peridotite xenoliths from the North China craton. Earth Planet. Sci. Lett. 288, 475–482.
Yang, W., Teng, F.-Z., Zhang, H.-F., Li, S.-G., 2012. Magnesium isotopic systematics of continental basalts from the North China craton: implications for tracing subducted carbonate in the mantle. Chem. Geol. 328, 185–194.
Yasuda, A., Fujii, T., Kurita, K., 1994. Melting phase relations of an anhydrous mid-ocean ridge basalt from 3 to 20 GPa: implications for the behavior of subducted oceanic crust in the mantle. J. Geophys. Res., Solid Earth 99, 9401–9414.
Young, E.D., Galy, A., 2004. The isotope geochemistry and cosmochemistry of magnesium. Rev. Mineral. Geochem. 55, 197–230.
Young, E.D., Tonui, E., Manning, C.E., Schauble, E., Macris, C.A., 2009. Spinel-olivine magnesium isotope thermometry in the mantle and implications for the Mg isotopic composition of Earth. Earth Planet. Sci. Lett. 288, 524–533.
Zeng, G., Chen, L.-H., Xu, X.-S., Jiang, S.-Y., Hofmann, A.W., 2010. Carbonated mantle sources for Cenozoic intra-plate alkaline basalts in Shandong, North China. Chem. Geol. 273, 35–45.
Zhang, G.-L., Chen, L.-H., Li, S.-Z., 2013. Mantle dynamics and generation of a geochemical mantle boundary along the East Pacific Rise – Pacific/Antarctic ridge. Earth Planet. Sci. Lett. 383, 153–163.
Zhang, G., Smith-Duque, C., Tang, S., Li, H., Zarikian, C., D'Hondt, S., Inagaki, F., 2012. Geochemistry of basalts from IODP site U1365: implications for magmatism and mantle source signatures of the mid-Cretaceous Osbourn Trough. Lithos 144–145, 73–87.
Zindler, A., Hart, S., 1986. Chemical geodynamics. Annu. Rev. Earth Planet. Sci. 14, 493–571.